Fringe shifts in multiple-beam Fizeau interferometry

John R. Rogers

Optical Sciences Center, University of Arizona, Tucson, Arizona 85721

Received August 7, 1981; revised manuscript received January 7, 1982

A computer program was developed to compute the profile of multiple-beam Fizeau fringes and was tested against laboratory observations. By using the program as a tool for studying the behavior of the fringes, a simplified model of the fringe formation process was developed. The shifts of the fringes from their expected locations are caused primarily by a reduction in spatial frequency that is due to the oblique projection of the fringes onto the detector. The angle at which the fringes are inclined to the input beam of the interferometer may be calculated by using a phase law developed by Brossel [Proc. Phys. Soc. **59**, 224 (1947)] and is independent of the reflectivity of the cavity. Once the orientations of the fringe planes and the detector are known, the fringe shifts may be calculated by using simple trigonometry. Although the absolute shift of a particular fringe may be an appreciable fraction of a fringe spacing, neighboring fringes have nearly identical shifts, making the relative fringe shift inconsequential. The finesse of the fringes may be increased by either tilting the Fizeau cavity or defocusing the detector optics. Unlike the tilt angle required to minimize the fringe shift, the tilt angle that maximizes the finesse is a strong function of the cavity reflectivity.

INTRODUCTION

It has long been known that multiple-beam Fizeau fringes do not exhibit the symmetry and degree of finesse characteristic of Fabry–Perot fringes because of the tendency of the higher-order beams to walk in the direction of the wide end of the wedge. An expression governing the relative phases of the beams was developed by Brossel,[1] but computing the fringe profile still required the summation of a great number of beams. Kinosita,[2] in 1952, laboriously performed this sum, obtaining a fringe profile for one particular wedge arrangement. More recently, Hall[3] constructed a computer model for performing the summation.

It is the modern high-speed computer that permits the shape and location of a multiple-beam fringe to be computed and the dependence of these on the various parameters of the system to be studied. In this paper, a model for computing the profile of a transmission Fizeau fringe is described, and its output is verified quantitatively against experimental results. The computer model is then applied as a tool for studying the shifts of the fringes from the traditional expectation that they be located at the positions where the Fizeau wedge is an integral number of half-wavelengths thick. A simplified model of the fringe formation process is developed, and it is shown to predict accurately the locations of the fringes. The concept of fringe sharpening, introduced by Langenbeck,[4] is also studied.

COMPUTATIONAL MODEL

The intensity profile of the fringe is formed point by point in the image plane by adding the complex amplitudes of the beams as they emerge from the wedge, as shown in Fig. 1. The jth-order beam, having experienced two transmissions and $2j$ reflections, has a magnitude (relative to an input beam of unit amplitude) given by

$$|A_j| = TR^j, \tag{1}$$

where T and R represent the intensity transmission and reflection coefficients, respectively.

The error involved in truncating the infinite summation after some finite number of beams may be estimated by making the pessimistic assumption that all the terms left out of the sum are exactly in phase with one another, thereby ensuring that the estimated error exceeds the actual error. The error caused by truncating the series after n terms then becomes an infinite geometric series with the summation index beginning at $n + 1$. This series may be expressed as the difference between an infinite series beginning at one and a finite series beginning at one and ending at n. By using the analytic solutions for these last two sums, the intensity error may be shown to be

$$\Delta I = \left(\frac{T}{1-R}\right)R^{2n+2}.$$

For simplicity, the assumption is made that there is no absorption (a good approximation, if dielectric mirrors are used), so the factor of $T^2/(1-R)^2$ becomes unity. The above expression may be inverted to produce the number of beams required for a given accuracy in the sum

$$n = \frac{\log(\Delta I)}{2\log(R)} - 1. \tag{2}$$

In this expression, it is convenient to use base-10 logarithms, so that the effect of changing the allowed intensity error ΔI by an order of magnitude can readily be seen.

With the modulus of each beam given by Eq. (1), and the number of beams required given by Eq. (2), only the relative phases of the beams remain to be computed. This will be done according to the method described by Brossel. As shown in Fig. 2, an input wave front drawn through the apex angle of a wedged pair of mirrors will be imaged into a family of wave fronts fanned out about the apex, the angle between any two wave-front images being twice the angle of the wedge. This is true regardless of the orientation of the wedge relative to

0030-3941/82/050638-06$01.00

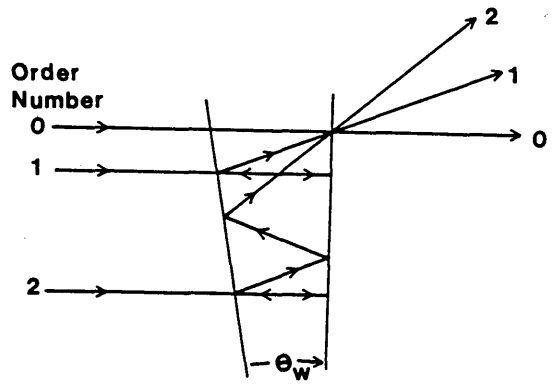

Fig. 1. Interference of three beams emerging from a Fizeau wedge.

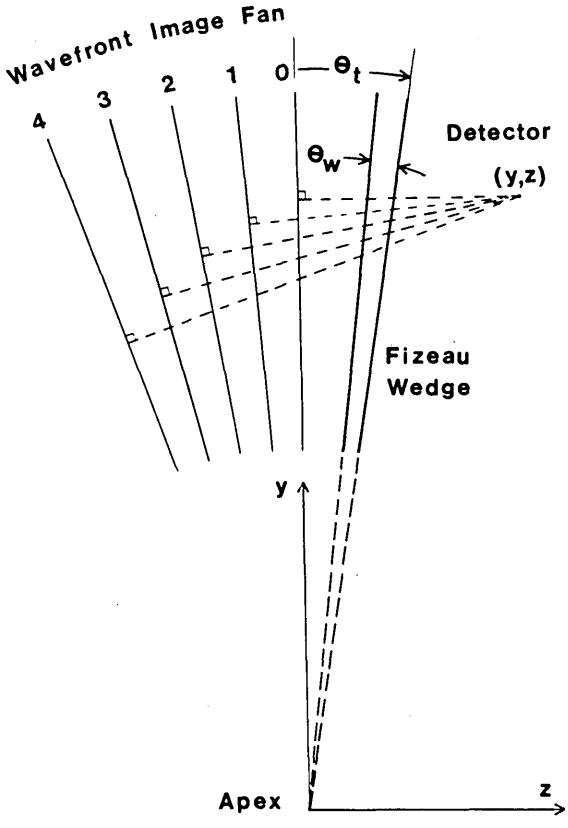

Fig. 2. Fan of wave-front images produced by a wedge.

the input wave front. Because these wave fronts are all images of one another, they have the same relative phase, and so their phases at the detector plane may be computed simply by propagating them along their normals to the detector. Simple trigonometry shows that the path length from the jth wave front to the detector at position (z, y) is given by

$$OPL_j = y \sin(2j\theta_w) + z \cos(2j\theta_w), \quad (3)$$

where z, y, and θ_w are as seen in Fig. 2. The phase of the jth beam is computed directly from the path length and makes use of the fact that the beam angle increases by $2j\theta_w$ each time the beam number j is increased. Considerable computational savings are gained by computing the sine and cosine of $2\theta_w$ once and then computing the values for the higher-order angles recursively.

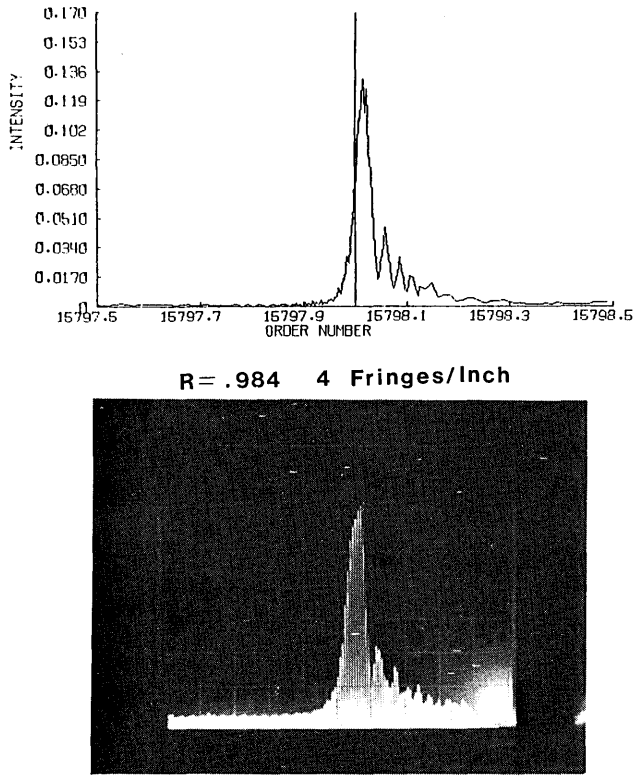

Fig. 3. Computed and observed fringe profiles; normal incidence.

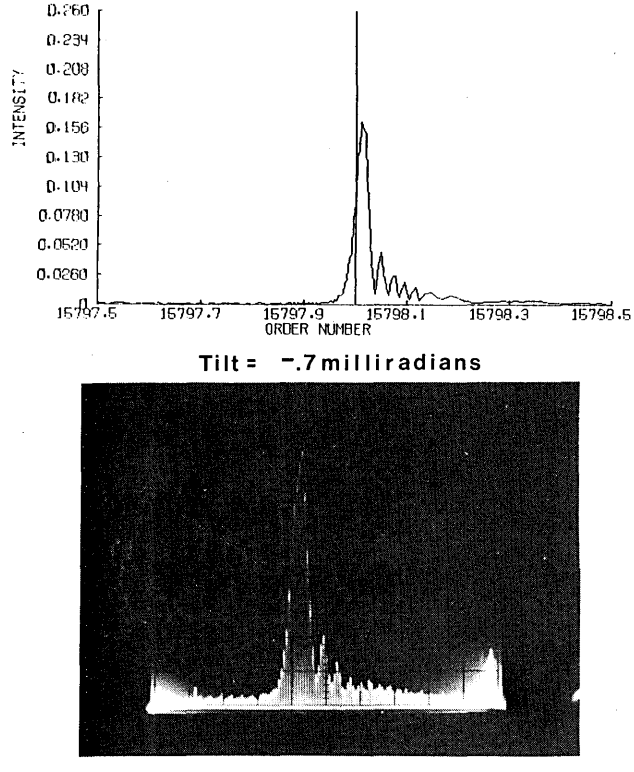

Fig. 4. Computed and observed fringe profiles, wedge tilted −0.7 mrad.

EXPERIMENTAL VERIFICATION

The ability of the program to predict fringe profiles was checked by setting up a Fizeau interferometer and imaging

the fringe patterns onto a linear photodiode array. The Fizeau wedge was formed by an air gap of about 4 mm between two dielectric mirrors. The intensity reflectivities of the mirrors at a wavelength of 514.5 nm were measured to be between 98 and 99%. In all cases reported here, the wedge angle was 0.04 mrad, giving a fringe spacing of 6.4 mm per fringe. A reflectivity of 98.4% was assumed in all computer simulations. Figure 3 compares the computed and actual profiles for the case in which the input beam is normal to the second mirror surface. In order to show the shift of the fringe from its expected location, a vertical line has been drawn through the computer plot at the point where the wedge is an integral number of half-wavelengths thick.

As Langenbeck points out, the fringe may be sharpened somewhat by tilting the Fizeau wedge slightly with respect to the incoming beam. To verify this aspect of the computer model, the experimental apparatus was rotated slightly, until a sharpening of the fringes was observed. The tilt angle was determined interferometrically, and this value was used to compute a fringe profile by using the computer model. Figure 4 shows the agreement between the computed and actual profiles.

Confidence in the accuracy of the program is essential because the fringe shifts described analytically in the next section are difficult, if not impossible, to measure experimentally.

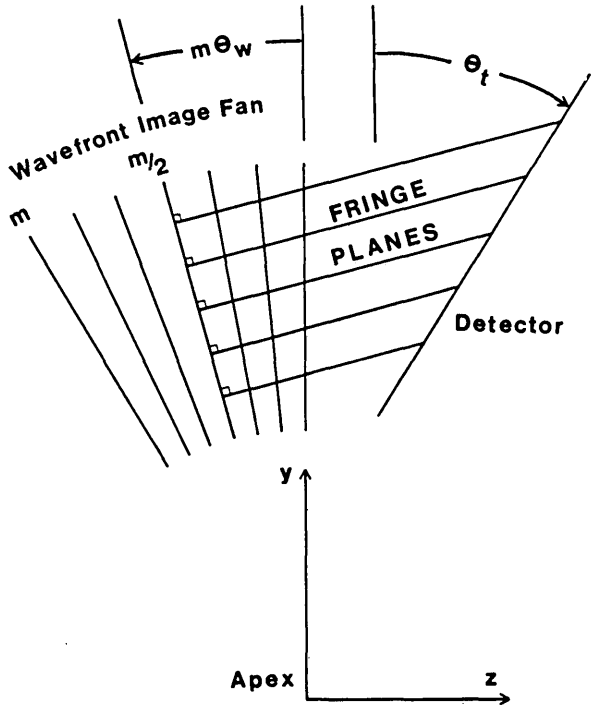

Fig. 5. Inclination of fringe planes that is due to contribution from many orders of beams.

SHIFTS OF THE FRINGE MAXIMA

An important feature of the wave-front images of Fig. 2 is that their orientations do not depend on the orientation of the wedge itself; the zeroth-order (unreflected) wave front will always be normal to the input beam, and each successive beam will be inclined at twice the wedge angle from the preceding wave front. Because the interference fringes produced by two wave fronts bisect the angle between the wave-front normals, the interference fringes produced by the fan of wave-front images must be inclined somewhat with respect to the input beam. For low reflectivities, only the first few wave-front images contribute significantly to the interference pattern, and the fringes will be essentially normal to the zeroth-order wave front. For high reflectivities, the contribution to the fringe pattern from the higher-order (higher-angle) wave fronts become significant, causing the fringes to be somewhat inclined. The amount that the fringes are inclined may be computed by comparing the phase law for the Fizeau fringes with that for the Fabry–Perot interferometer. Brossel derived an approximate expression for Eq. (2) by assuming that the detector would be placed on the zeroth-order wave front (setting z to zero) and expanding the trigonometric functions. It is only a slight extension to assume instead that the detector be located on the nth wave front (n arbitrary) and compute the optical path length from the jth wave front to the nth. Not surprisingly, the optical path length depends only on the difference of j and n, not on their individual values:

$$OPL_{j,n} = (y^2 + z^2)^{1/2}\{\sin[2(j - n)\theta_w]\}.$$

At this point it is convenient to represent the difference in the order numbers j and n by the number m, and, after the sine is expanded, the expression becomes

$$OPL_m \simeq 2mt - 4/3t\theta_w{}^2m^3, \quad (4)$$

where t is the thickness of the wedge. Recognizing that the term linear in m is exactly the optical path length for a Fabry–Perot interferometer, the cubic term may be viewed as an error term. If the error term for a pair of wave fronts exceeds half a wavelength, then the interference of those two wave fronts will degrade, rather than sharpen, the fringes produced by the wave fronts of less separation in order. This fact amounts to a restriction of the number of consecutive wave fronts that can interfere in a constructive manner and will be referred to as Brossel's criterion:

$$m^3 \leqslant \frac{3\lambda}{8t\theta_w{}^2}. \quad (5)$$

This expression indicates that *any* set of m consecutive wave fronts is phased so as to produce sharp fringes; however, the first (lowest-order) m fringes in the fan have the greatest amplitude and therefore dominate. For the purpose of obtaining a simple, if approximate, expression governing fringe shifts, it is convenient to make the approximation that the first m wave fronts contribute equally to the fringes and that the remaining wave fronts only contribute noise. The effective wave front is now symmetric about the wave front of order $m/2$, and the fringes produced must be normal to that wave front, which is inclined at an angle of $m\theta_w$ from the zeroth-order wave front. This is shown in Fig. 5. (That m might be odd and that the wave front of order $m/2$ might not exist is immaterial; it is only the angle of the plane of symmetry that is of interest.)

The inclination of the fringes will produce two distinct effects that will manifest themselves as a shift of the fringes from their expected location. The first is a uniform shift of the fringe pattern across the detector, and the other is a change in the fringe spacing, in which the zero-order fringe remains at the apex of the wedge and the higher-order fringes expand

outward. The latter effect is of more consequence and will be treated first.

The change in the spatial frequency results simply from the oblique projection of the fringes onto the detector. If the detector is tilted by an angle θ_t with respect to the normal to the input beam, then the angle between the fringes and the detector normal is given by the difference between the fringe angle $m\theta_w$ and the detector angle θ_t. (The sign convention used in the figures is that counterclockwise rotations are represented by positive angles.) The detected spatial frequency is reduced from the actual spatial frequency by the cosine of the obliqueness angle:

$$\xi_d = \xi \cos(m\theta_w - \theta_t).$$

Here, ξ represents the actual spatial frequency, as would be measured in a plane normal to the fringes. The distance of any fringe from the wedge apex is simply its order number divided by the spatial frequency, so the shift S along the detector that is due to the change in spatial frequency is given by

$$S = \left(\frac{\text{order}}{\xi}\right)\left[\frac{1}{\cos(m\theta_w - \theta_t)} - 1\right].$$

It is often more useful to measure the shift in units of fringes rather than in units of linear measure. In this case, the shift is

$$S = (\text{order})\left[\frac{1}{\cos(m\theta_w - \theta_t)} - 1\right]. \tag{6}$$

Because the cosine factor can only reduce the spatial frequency, a fringe of a given order may only move away from the apex, and the shift vanishes only if the tilt angle of the detector is the same as that of the $m/2$-order wave front. In almost all interferometric situations, the cosine factor is nearly equal to one, reducing the second factor of Eq. (6) nearly to zero. This can be offset by a large order number, which is the thickness of the cavity measured in half-wavelengths. Although the overall shift given by Eq. (6) may indeed be an appreciable fraction of a fringe spacing, it is important to realize that the neighboring fringes have nearly identical shifts, so that the shift of a given fringe, *relative to its neighbors*, is generally quite small. In the usual case in which only this relative shift is important, the order number of Eq. (6) should be replaced with the number of fringes visible across the pupil of the interferometer.

Although Eq. (6) accounts for the spatial-frequency change that is due to the obliqueness of the fringes to the detector, Fig. 5 shows that moving the detector (or its image) along the axis of the input beam will produce a uniform shift of the entire fringe pattern. The law of sines shows that the shift S along the detector that is due to defocusing the detector image an amount Δz is given by

$$S = \frac{\Delta z \sin m\theta_w}{\cos(m\theta_w - \theta_t)}.$$

This shift may be put in terms of fringes, instead of units of linear measure, by multiplying by the spatial frequency:

$$S = \frac{\xi \Delta z \sin m\theta_w}{\cos(m\theta_w - \theta_t)}. \tag{7}$$

Because this is a uniform shift of the fringes, it is of no consequence unless an absolute measure of the fringe position is required.

It is somewhat surprising that these expressions for the fringe shifts do not depend on the reflectivity. The only dependence on the reflectivity lies in the assumption that it is Brossel's criterion, and not the reduction of beam intensity with order number, that limits the useful interference.

To test the accuracy of these predictions, fringe profiles were computed for several combinations of reflectivity, wedge angle, and detector tilt angle. Figure 6 shows the absolute shift of the fringe peak as a function of detector tilt angle for a 4-mm-thick wedge of reflectivity 0.90, with a wedge angle of 0.04 mrad. The error bars correspond to the sample spacing of the points in the fringe profile and represent the accuracy to which the location of the fringe peak is known. The theoretical curve, given by Eq. (6), demonstrates the general trend of the shift phenomenon and accurately predicts the tilt angle at which the shift is a minimum. Note also that the shifts are quite small, even though the order number in this case is about 16,000. The relative shift across, for instance, ten fringes would be a factor of 1600 less. To test the prediction that the fringe shift would be independent of the reflectivity, similar plots were generated for reflectivities of 0.95 and 0.984, which are shown in Figs. 7 and 8, respectively. Even in the high-reflectivity case, in which the fringe profile is strongly degraded, the theoretical curve accurately predicts the position of the minimum shift, if not the amount of the shift.

FRINGE SHARPENING

In the preceding section, it was stated that the orientation of wave-front fan is independent of the orientation of the wedge.

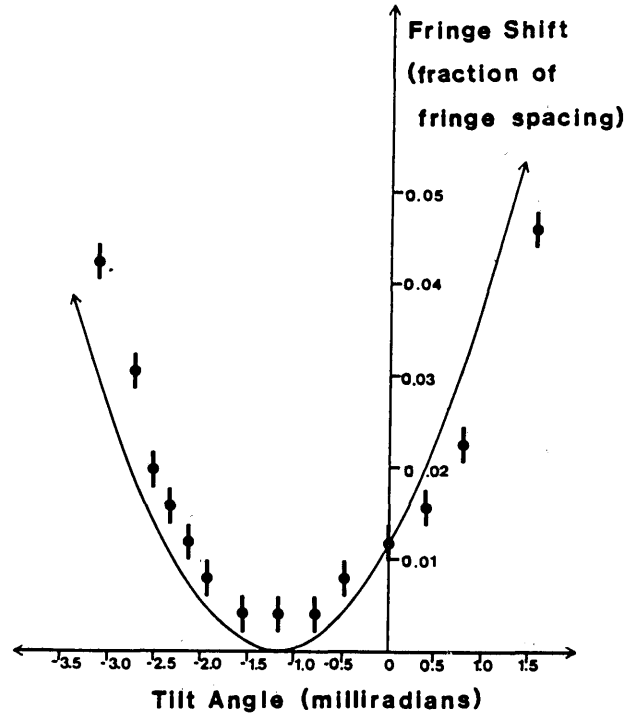

Fig. 6. Fringe shift as a function of detector tilt angle; intensity reflectivity, 0.90.

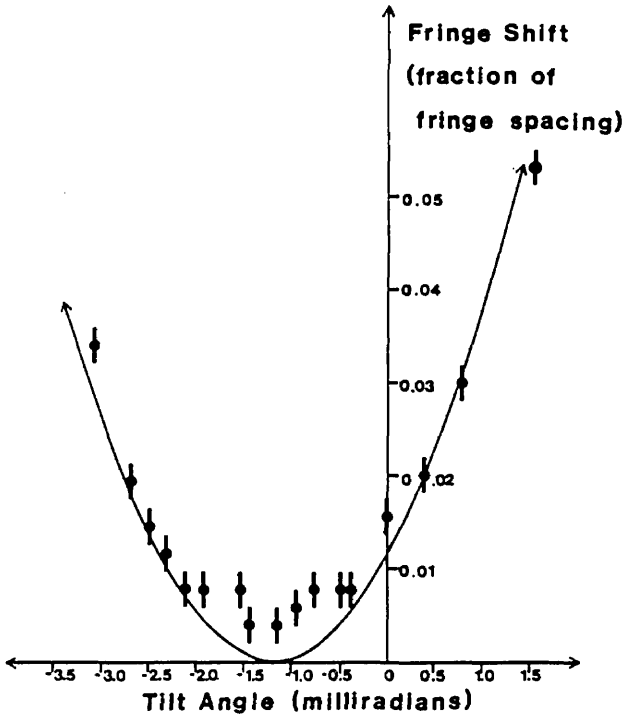

Fig. 7. Fringe shift as a function of detector tilt angle; intensity reflectivity, 0.95.

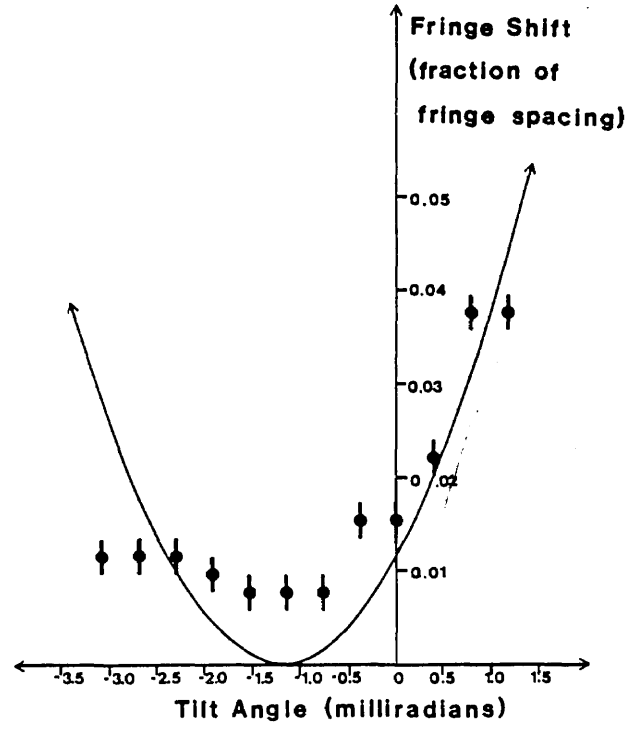

Fig. 8. Fringe shift as a function of detector tilt angle; intensity reflectivity, 0.984.

This is not true of the *position* of the fan, for the wave fronts (and in particular the zeroth-order wave front) must pass through the apex of the wedge. Tilting the wedge causes the apex to swing in an arc, and in so doing, causes the entire wave-front fan to move with it; however, the detector remains fixed in its position, and the net result is that the detector has been displaced either into or away from the wave-front fan, depending on the direction of tilt. Once this is understood, it is clear that this same effect may be achieved by simply translating the detector, or defocusing the detector imaging optics, by an amount equal to but opposite the amount through which the fan moved when the wedge was tilted. (This is strictly true only if the detector does not tilt when the Fizeau wedge is tilted. If, on the other hand, the detector or its image remains fixed on the rear wedge surface as the wedge is tilted, then the detector has been tilted as well as translated.)

Because of the smallness of the wedge angle, the distance along the wedge from the illuminated part to its apex can be quite large, and even a small tilt of the wedge may correspond to a considerable amount of defocus. As an example, the 0.7 mrad of tilt introduced in Fig. 4 corresponds to a longitudinal displacement of 7.1 cm. (Computer simulation using this amount of defocus yields a curve exactly like that of Fig. 4 except for the transverse shift of the previous section.)

The importance of this translation is that the detector may be placed inside the wave front, in a position of greater symmetry. If the detector were imaged onto one of the wave fronts in the fan, then any two wave fronts symmetrically located about it would have exactly the same optical path lengths to it.

It was previously mentioned that the shift of the fringes may be minimized by tilting the detector to be parallel to the wave front of order $m/2$, m being given by Eq. (5). If this tilt were produced not by tilting the detector but by tilting the wedge and keeping the detector imaged onto its rear surface, the result is that the detector is exactly imaged onto the $m/2$-order wave front. The first m wave fronts in the fan are then symmetrically oriented about the detector, and one might expect that that condition would produce the sharpest fringes, but it simply does not. Figure 9 shows the finesse of com-

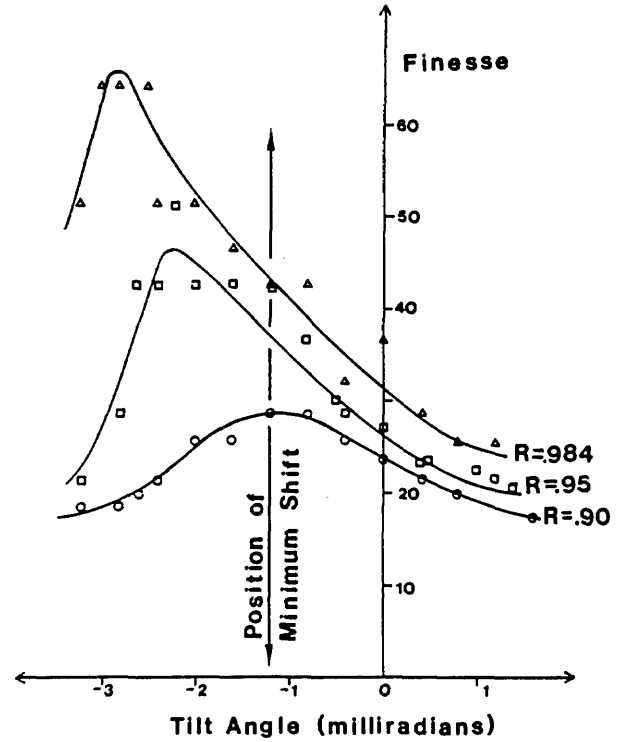

Fig. 9. Finesse as a function of tilt angle of wedge for three reflectivities.

puter-simulated fringe profiles as a function of the tilt angle θ_t for the reflectivities 0.90, 0.95, and 0.984. (The finesse was taken to be the ratio of the fringe spacing to the full width at half-maximum *of the primary peak*, ignoring the presence of the secondary maxima. The uncertainty in the finesse that is due to the sampling interval across the fringe is approximately 10%.) The solid curves in the figure have been hand drawn to fit the computer-simulated data. The figure clearly shows that minimum fringe shift and maximum finesse do not occur at the same tilt angle of the wedge; furthermore, the former is independent of the reflectivity, and the latter is not.

Langenbeck proposed a method for computing the tilt angle required for maximum finesse, based on the idea of equalizing the phase errors on the left- and right-hand sides of the fan.[4] The result was that the detector should be imaged onto the wave front whose order number is 0.8 times the total number of wave fronts contributing appreciably to the interference, the latter being obtained from the formula

$$n = 3/(1 - r).$$

[A comparison of this formula with Eq. (2) shows that this assumes an intensity error of about 0.002.] For reflectivities of 0.90, 0.95, and 0.984, this scheme yields tilt angles of −2.4, −4.8, and −15 mrad, respectively, each far in excess of the tilt angle that actually maximizes the finesse.

CONCLUSIONS

The shifts of multiple-beam fringes from their expected locations are due for the most part to the oblique projection of the fringes onto the detector and are practically independent of reflectivity. The angle at which the fringes recline, and the angle at which the detector must be tilted to minimize the shift, may be computed simply by using Brossel's criterion. For a given detector orientation, an estimate of the shift may be obtained by using simple trigonometric calculations. Sample computations indicate that in most interferometric applications, in which only relative fringe positions are measured, these shifts are inconsequential. The tilt angle that maximizes the finesse of the fringes is a strong function of the reflectivity, unlike the angle that minimizes the shift of the fringes.

REFERENCES

1. J. Brossel, "Multiple-beam localized fringes: intensity distribution and localization," Proc. Phys. Soc. London **59**, 224–234 (1947).
2. K. Kinosita, "Numerical evaluation of the intensity curve of a multiple-beam Fizeau fringe," J. Phys. Soc. Jpn. **8**, 219–225 (1953).
3. T. A. Hall, "Fizeau interferometer profiles at finite acceptance angles," J. Phys. E. **2**, 837–840 (1969).
4. P. Langenbeck, "Fizeau interferometer-fringe sharpening," Appl. Opt. **9**, 2053–2058 (1970).